HIERARCHY OF NUMERICAL SCHEMES FOR THE BIE SOLUTION IN 2D FLOW SIMULATION USING VORTEX METHODS

YULIA IZMAILOVA, ILIA MARCHEVSKY & KSENIIA SOKOL
Bauman Moscow State Technical University, Russia

ABSTRACT

The problem of 2D incompressible flow simulation around airfoils with sharp edges and corner points is considered. The solution of the boundary integral equation with respect to vortex sheet intensity, arising in Lagrangian vortex method, has weak singularity that cannot be resolved correctly in the framework of the existing Galerkin-type numerical schemes. Known numerical schemes with piecewise-constant or piecewise-linear numerical solution representation provide solution reconstruction with high quality and the second order of accuracy only for piecewise-smooth bounded solutions. For singular solutions their order of accuracy goes down to the first. It is shown that wrong behaviour of numerical solution takes place only on the panels that adjust to the corner point. Modified numerical scheme is developed that is based on the Galerkin–Petrov approach and allows us to obtain integral characteristics of solution (the components of the added masses tensor) with the second order of accuracy. The scheme can be easily implemented in codes developed for flow simulations using the vortex particle method.

Keywords: vortex methods, boundary integral equation, unbounded solution, added mass tensor.

1 INTRODUCTION

Vortex methods of computational fluid mechanics [1] have rather narrow range of applicability: they are suitable for incompressible one-phase isothermal flows simulation. However, they are widely used in engineering applications [2], [3], especially connected with estimation of hydrodynamic loads acting on structures. Reviewing their advantages briefly, the following features should be pointed out:

- external and unbounded flows can be simulated with exact satisfaction of the perturbations decay boundary condition at infinity.
- efficient coupling schemes are developed that allow for solving fluid–structure interaction (FSI) problems with arbitrary translations, rotations, and deformations of the streamlined surface.
- the most part of computational resources is ‘concentrated’ in the part of the flow domain with non-zero vorticity; such area is usually rather compact.
- vortex methods belong to a class of particle-based methods, where Lagrangian particles are considered as vorticity carriers; it follows therefore that vortex methods provide rather small numerical diffusion.

Note that a wide list of investigations that are devoted to the problems connected with the vorticity field evolution simulation in the flow domain can be cited, and more or less efficient and accurate algorithms are developed that allow for simulation of vorticity convective transfer and its viscous diffusion. At the same time, the problems connected to the streamlined body (airfoil) simulation are investigated much poorly. In major part of papers and monographs only some general words can be found, mainly pointing out that the problem of the airfoil simulation is equivalent to the solving of some boundary integral equation (BIE) with respect to double layer potential density, vortex sheet intensity or vortex flux intensity.

WIT Transactions on Engineering Sciences, Vol 135, © 2023 WIT Press
www.witpress.com, ISSN 1743-3533 (on-line)
doi:10.2495/BE460141

And it is mentioned usually that the BIE can be solved using the same approaches as applied in the framework of the boundary element method. At the same time, the results of the accuracy investigation of the known numerical schemes that can be applied in 2D problems being solved by vortex methods, show that the error can be high enough, and it can be the most significant cause that bounds the accuracy of the flow simulation in the whole.

In the present paper, the approach is suggested that allows for increasing the accuracy of the BIE solution significantly for the airfoils with sharp edge or corner point, where the exact solution has the singularity.

2 THE GOVERNING EQUATION

We consider an approach to incompressible flow around an airfoil simulation, according to which it is necessary to solve the BIE with respect to vortex sheet intensity. For simplicity let us assume that the flow domain F is infinite and bounded only by the considered airfoil, and there is some known vorticity distribution $\Omega(\boldsymbol{\xi})$, $\boldsymbol{\xi} \in F$, in the flow.

Then, the unknown vortex sheet intensity $\gamma(\mathbf{r})$ satisfies the vector boundary integral equation that arises from the no-slip condition satisfaction on the airfoil surface line:

$$\oint_K \frac{\mathbf{k} \times (\mathbf{r} - \boldsymbol{\xi})}{2\pi |\mathbf{r} - \boldsymbol{\xi}|^2} \gamma(\boldsymbol{\xi}) dl_\xi - \alpha(\mathbf{r}) \gamma(\mathbf{r}) \boldsymbol{\tau}(\mathbf{r}) = \mathbf{f}(\mathbf{r}), \qquad \mathbf{r} \in K, \tag{1}$$

where K is the airfoil surface line; $\mathbf{k}$ is a unit vector orthogonal to the flow plane; $\alpha(\mathbf{r})$ is equal to the outer angle at the corresponding point divided by 2π (so, on smooth parts of the airfoil boundary $\alpha = 1/2$); $\boldsymbol{\tau}(\mathbf{r})$ is tangent unit vector defined such as $\mathbf{n}(\mathbf{r}) \times \boldsymbol{\tau}(\mathbf{r}) = \mathbf{k}$, $\mathbf{n}(\mathbf{r})$ is outer normal unit vector; the right-hand side is expressed as follows:

$$\mathbf{f}(\mathbf{r}) = -\Bigg(\mathbf{V}_\infty + \int_F \frac{\mathbf{k} \times (\mathbf{r} - \boldsymbol{\xi})}{2\pi |\mathbf{r} - \boldsymbol{\xi}|^2} \Omega(\boldsymbol{\xi}) dS_\xi + \\ + \int_K \frac{\mathbf{k} \times (\mathbf{r} - \boldsymbol{\xi})}{2\pi |\mathbf{r} - \boldsymbol{\xi}|^2} \gamma^{att}(\boldsymbol{\xi}) dl_\xi + \int_K \frac{\mathbf{r} - \boldsymbol{\xi}}{2\pi |\mathbf{r} - \boldsymbol{\xi}|^2} q^{att}(\boldsymbol{\xi}) dl_\xi - \alpha(\mathbf{r}) \mathbf{V}_K(\mathbf{r}) \Bigg),$$

where $\mathbf{V}_\infty$ is incident velocity; $\gamma^{att}(\boldsymbol{\xi})$ and $q^{att}(\boldsymbol{\xi})$ are the so-called attached vortex and source sheet intensities, which are determined as tangent and normal components of the airfoil surface line velocity $\mathbf{V}_K(\mathbf{r})$, respectively:

$$\gamma^{att}(\boldsymbol{\xi}) = \mathbf{V}_K(\boldsymbol{\xi}) \cdot \boldsymbol{\tau}(\boldsymbol{\xi}), \qquad q^{att}(\boldsymbol{\xi}) = \mathbf{V}_K(\boldsymbol{\xi}) \cdot \mathbf{n}(\boldsymbol{\xi}).$$

Note that in case of immovable airfoil the last three terms in the expression for the right-hand side are equal to zero; the assumption about the absence of the other surfaces in the flow is not essential; in order to take it into account, one should consider the system of the BIEs.

Traditionally, the following approach to numerical solution of eqn (1) is applied: firstly, it is projected onto the normal unit vector $\mathbf{n}(\mathbf{r})$, as the result, one obtains a singular BIE of the first kind with the Hilbert-type kernel $P_n(\mathbf{r}, \boldsymbol{\xi})$:

$$\oint_K \underbrace{-\frac{\boldsymbol{\tau}(\mathbf{r})\cdot(\mathbf{r}-\boldsymbol{\xi})}{2\pi|\mathbf{r}-\boldsymbol{\xi}|^2}}_{P_n(\mathbf{r},\boldsymbol{\xi})}\gamma(\boldsymbol{\xi})\,dl_\xi = \mathbf{f}(\mathbf{r})\cdot\mathbf{n}(\mathbf{r}), \qquad \mathbf{r}\in K. \tag{2}$$

For its solution special quadrature formulae are used (usually, similar to central quadratures rule) that allows for estimating the Cauchy principal value of the corresponding integrals. The family of such numerical schemes we call hereinafter N-scheme. Detailed investigation of such schemes with the proof of their convergence can be found in Lifanov [4] and Lifanov et al. [5].

Another approach leads to the so-called T-schemes and starts with the projection of eqn (1) onto tangent unit vector $\boldsymbol{\tau}(\mathbf{r})$ [6]. This means that it is necessary to solve the BIE of the second kind with bounded kernel (in case of smooth airfoil) or absolutely integrable kernel (in case of airfoils with sharp edges or corner points) $P_\tau(\mathbf{r},\boldsymbol{\xi})$:

$$\oint_K \underbrace{\frac{\mathbf{n}(\mathbf{r})\cdot(\mathbf{r}-\boldsymbol{\xi})}{2\pi|\mathbf{r}-\boldsymbol{\xi}|^2}}_{P_\tau(\mathbf{r},\boldsymbol{\xi})}\gamma(\boldsymbol{\xi})\,dl_\xi - \alpha(\mathbf{r})\gamma(\mathbf{r}) = \mathbf{f}(\mathbf{r})\cdot\boldsymbol{\tau}(\mathbf{r}), \qquad \mathbf{r}\in K. \tag{3}$$

For such an equation the family of more accurate numerical schemes can be developed; they are mostly based on the Galerkin approach.

3 SMOOTH AND NON-SMOOTH AIRFOILS

Let us firstly touch the case of smooth airfoil. The solution of the BIE here is smooth enough, and it can be reconstructed in principally without significant issues. We note only that the implementation of the above mentioned T-schemes may be non-trivial and requires rather accurate integrals computation that arise in Galerkin-type procedure [7].

Theoretic estimates, proven by numerical computations, show that the accuracy of numerical solution depends on the airfoil surface line discretization way. If it is replaced by a polygon consisting of straight panels, the order of accuracy (in L_1 norm) cannot be higher than the second: the first order of accuracy is achieved for piecewise-constant solution representation, the second order of accuracy – for piecewise-linear distribution of the vortex sheet intensity [8]. In much more complicated schemes, where the curvilinearity of the panels is taken into account explicitly [9], the third order of accuracy can be achieved at piecewise-quadratic numerical solution representation.

So, one can conclude that the problem of higher-order numerical schemes development is solved, more or less, for smooth airfoils.

At the same time, when one deals with the airfoil with sharp edge (i.e., Joukowsky wing) or corner points (i.e., rectangular or semicircular), the situation becomes more dramatic.

Let us firstly examine the case of Joukowsky wing airfoil (or some similar one). Initially, we note that the BIE (1), as well as its projections onto the normal and tangent directions (2) and (3), has infinite set of solutions. In order to pick out the unique solution, it is necessary, as a rule, to specify the total value of vorticity that is contained in the vortex sheet,

$$\oint_K \gamma(\boldsymbol{\xi})\,dl_\xi = \Gamma, \tag{4}$$

or, the same, to specify the velocity field circulation around the airfoil.

It is well-known that for wing airfoil there exists some particular value of circulation Γ^* that corresponds to the Chaplygin–Joukowsky condition, known also as Kutta condition, according to which the flow velocity remains finite at the sharp edge [10] (note that this condition is also applicable to a wider class of the airfoils with single corner points, e.g., the so-called generalized Joukowsky airfoils [11]). In this case, the solution of the BIE eqn (1) remains bounded and can have only jump discontinuity at the mentioned point (Fig. 1). For such solutions the above mentioned numerical schemes remain suitable, and they provide (sometimes with some obvious limitations) the same order of accuracy as for smooth solutions.

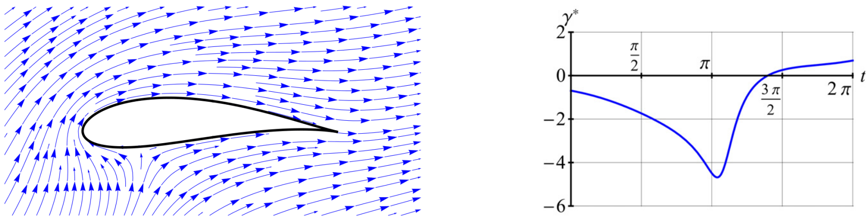

(a) (b)

Figure 1: (a) Flow around Joukowsky wing airfoil satisfying the Chaplygin–Joukowsky condition; and (b) Vortex sheet intensity with respect to a parameter that varies from 0 to 2π along the airfoil surface line.

However, the Chaplygin–Joukowsky condition corresponds to the steady-state flow regime that can be interesting in some cases, but such approach is not applicable to unsteady flows simulation, for example, when it is necessary to simulate transient regimes, etc. In this case, the circulation value Γ depends only on angular acceleration of the airfoil (i.e., if it moves plane-parallel or with constant angular velocity, then $\Gamma = 0$). Thereby, for unsteady flows around the airfoils with edges or corner points the solution of the BIE eqn (1) becomes singular in the corresponding point (Fig. 2), and its asymptotic behavior is known [4]:

$$\gamma(s) \sim s^{-\mu}, \qquad \mu = 1 - \frac{\pi}{\chi'} \tag{5}$$

where s is the distance to the edge; χ is the outer angle at the edge point. Consequently, for the classical Joukowsky airfoil with sharp edge there will be singularity of $s^{-1/2}$ type; for corner points with finite inner angle it has type $s^{-\mu}$, $0 < \mu < 1/2$.

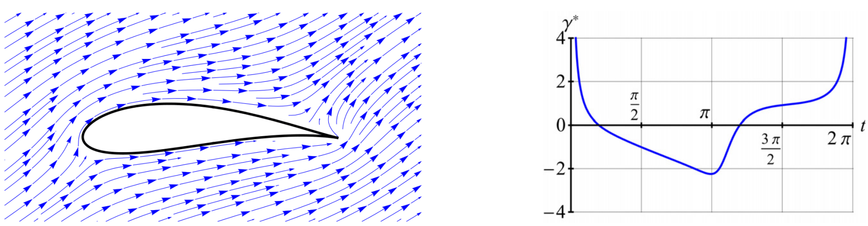

(a) (b)

Figure 2: (a) Flow around Joukowsky wing airfoil for $\Gamma = 0$; and (b) Vortex sheet intensity with respect to a parameter that varies from 0 to 2π along the airfoil surface line.

4 GALERKIN-TYPE NUMERICAL SCHEMES

In the above mentioned numerical schemes the Galerkin approach is implemented in order to derive the linear system that is the discrete analogue of the BIE.

The airfoil surface line K is replaced with the polygon consisting of the panels K_i, $i = 1, \ldots, N$. The solution is reconstructed as a combination of basis functions:

- for piecewise-constant solution representation

$$\gamma(\mathbf{r}) = \sum_{i=1}^{N} \gamma_i^0 \phi_i^0(\mathbf{r}), \qquad \mathbf{r} \in K, \tag{6}$$

- for piecewise-linear solution representation

$$\gamma(\mathbf{r}) = \sum_{i=1}^{N} \left(\gamma_i^0 \phi_i^0(\mathbf{r}) + \gamma_i^1 \phi_i^1(\mathbf{r}) \right), \qquad \mathbf{r} \in K, \tag{7}$$

where two families of basis functions are the following:

$$\phi_i^0(\mathbf{r}) = \begin{cases} 1, & \mathbf{r} \in K_i, \\ 0, & \mathbf{r} \notin K_i; \end{cases} \qquad \phi_i^1(\mathbf{r}) = \begin{cases} (\mathbf{r} - \mathbf{c}_i) \cdot \boldsymbol{\tau}_i / L_i, & \mathbf{r} \in K_i, \\ 0, & \mathbf{r} \notin K_i, \end{cases}$$

here $\mathbf{c}_i$ is the center of the panel K_i; L_i is its length.

In order to determine unknown coefficients γ_i^p values, the solution in the form (6) or (7) is substituted to the T-model (3), then the expression for the residual is multiplied by some projection function $\psi_i^p(\mathbf{r})$, and the result is assumed to be equal to zero. As the result, the algebraic linear system is obtained, from which the unknown coefficients are found.

The most obvious way is to choose the projection functions to be equal to basis ones; this corresponds to the classical Galerkin approach and for smooth airfoils (and, consequently, smooth and bounded solutions) can be considered as residual orthogonality condition in subspace of the L_2 functional space.

Such approach is implemented in Kuzmina and Marchevskii [7] where all necessary formulae for the integrals arising in the Galerkin procedure are presented. It works perfectly, providing the first and second orders of accuracy in case of smooth or at least bounded solutions in L_1 norm.

As an example, let us consider the problem of the added masses calculation. The added masses are widely used in various engineering applications in order to estimate the hydrodynamic forces acting the structure that moves in the flow with acceleration, i.e., vibrating in the flow. At the same time, according to Dynnikova [12] added mass tensor components also can be considered as integral characteristics of the vortex sheet intensity on the airfoil surface line that satisfies the BIE (1) or the equivalent eqns (2) and (3).

In order to estimate the added masses of the airfoil, three model problems should be considered: impulsive start of the airfoil in horizontal and vertical directions in still media with unit velocity $|\mathbf{V}_K| = 1$, and its impulsive start in rotational motion with unit angular velocity $\omega = 1$. The value of total circulation in additional condition (4) should be chosen as

$$\Gamma = -\oint_K \gamma^{att}(\boldsymbol{\xi})\, dl_\xi,$$

it is equal to zero except of rotational motion.

Then, the components of the added mass tensor for two-dimensional flow are calculated as follows [12]:

$$\lambda_{dx} = \oint_K \rho y\left(\gamma_d(\mathbf{r}) + \gamma_d^{att}(\mathbf{r})\right) dl_r, \qquad \lambda_{dy} = -\oint_K \rho x\left(\gamma_d(\mathbf{r}) + \gamma_d^{att}(\mathbf{r})\right) dl_r,$$

$$\lambda_{d\omega} = -\frac{1}{2}\oint_K \rho\left(x^2 + y^2\right)\left(\gamma_d(\mathbf{r}) + \gamma_d^{att}(\mathbf{r})\right) dl_r,$$

where x and y are the abscise and the ordinate of the point $\mathbf{r}$ at the airfoil boundary; index d has values x, y and ω and corresponds to the motion direction of the airfoil; $\gamma_d(\mathbf{r})$ and $\gamma_d^{att}(\mathbf{r})$ denote vortex sheets intensities in the airfoil motion in the d th direction; ρ is the flow density. The exact values are known for the added masses of the elliptic airfoil with semiaxes a and b [13]:

$$\lambda_{xx}^* = \rho\pi b^2, \quad \lambda_{yy}^* = \rho\pi a^2, \quad \lambda_{\omega\omega}^* = \frac{1}{8}\rho\pi\left(a^2 - b^2\right)^2, \quad \lambda_{xy}^* = \lambda_{x\omega}^* = \lambda_{y\omega}^* = 0\,.$$

In Table 1 relative error of the added masses computation is given (maximal value for all diagonal components) for the elliptic airfoil with 5:1 semiaxes ratio, which surface line is discretized into N panels of equal length. $\mathcal{T}^0$ and $\mathcal{T}^1$ denote numerical schemes with piecewise-constant and piecewise-linear solution representations. In brackets a'posteriori estimations for the order of accuracy are shown.

Table 1: Relative errors of the added mass tensor estimation for elliptical airfoil 5:1 semiaxes ratio for different number of panels.

N	100	200	400	800	1600	3200
$\delta(\mathcal{T}^0)$	$1.69\cdot10^{-2}$	$4.39\cdot10^{-3}$	$1.10\cdot10^{-3}$	$2.73\cdot10^{-4}$	$6.81\cdot10^{-5}$	$1.70\cdot10^{-5}$
Order	—	(1.94)	(2.00)	(2.01)	(2.01)	(2.00)
$\delta(\mathcal{T}^1)$	$9.16\cdot10^{-3}$	$2.52\cdot10^{-3}$	$6.48\cdot10^{-4}$	$1.64\cdot10^{-4}$	$4.11\cdot10^{-5}$	$1.03\cdot10^{-5}$
Order	—	(1.86)	(1.96)	(1.98)	(1.99)	(2.00)

One can see that the second order of accuracy takes place for both numerical schemes; the scheme $\mathcal{T}^1$ is 40% more accurate in comparison to $\mathcal{T}^0$. Note that the order of accuracy for the $\mathcal{T}^0$ scheme is higher than for vortex sheet intensity; this is due to the fact that the solution is smooth. For the $\mathcal{T}^1$ scheme the orders of accuracy are equal to 2 in both cases.

Now let us examine these schemes for Joukowsky wing airfoil [13] (Fig. 3).

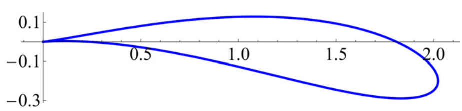

Figure 3: Joukowsky airfoil shape for the parameters $a = 1$, $\eta = 1.15$, $\alpha = \pi/30$.

The specific feature of this airfoil is that in horizontal motion at $\Gamma = 0$ in condition (4) the exact solution for vortex sheet intensity $\gamma(s)$, where s is arclength coordinate, is bounded and has jump discontinuity at the sharp edge (Fig. 4(a)).

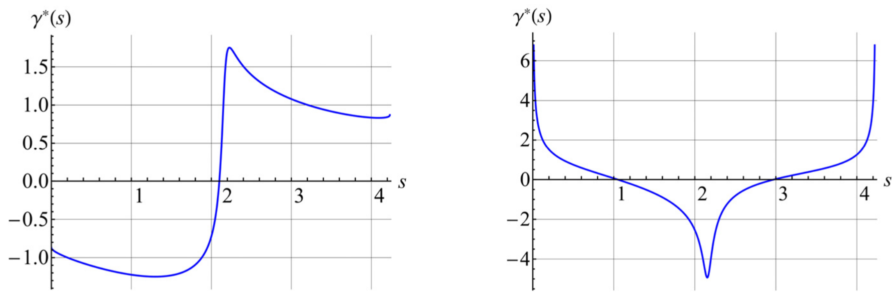

(a) (b)

Figure 4: Exact solution for the vortex sheet intensity $\gamma^*(s)$ for the Joukowsky wing airfoil in (a) horizontal; and (b) vertical motion. s is arc length measured along the airfoil surface line from the sharp edge.

The expressions for added mass tensor components for such airfoil could be found in Sedov [13].

In Table 2 maximal relative error of the added masses computation is given for λ_{xx}, $\lambda_{x\omega}$ and $\lambda_{y\omega}$ (the components that can be obtained after horizontal airfoil motion simulation) for the wing airfoil discretized into N panels of equal length. Again, in brackets a'posteriori estimations for the order of accuracy are shown.

Table 2: Relative errors of the added masses λ_{xx}, $\lambda_{x\omega}$ and $\lambda_{y\omega}$ estimation for Joukowsky wing airfoil for different number of panels.

N	100	200	400	800	1600	3200
$\delta(\mathcal{T}^0)$	$6.77 \cdot 10^{-3}$	$1.61 \cdot 10^{-3}$	$3.71 \cdot 10^{-4}$	$8.25 \cdot 10^{-5}$	$1.92 \cdot 10^{-5}$	$4.79 \cdot 10^{-6}$
Order	—	(2.07)	(2.12)	(2.17)	(2.10)	(2.00)
$\delta(\mathcal{T}^1)$	$4.55 \cdot 10^{-3}$	$1.18 \cdot 10^{-3}$	$2.99 \cdot 10^{-4}$	$7.50 \cdot 10^{-5}$	$1.88 \cdot 10^{-5}$	$4.70 \cdot 10^{-6}$
Order	—	(1.95)	(1.98)	(1.99)	(2.00)	(2.00)

Here we see that both schemes again provide the second order of accuracy and their errors are nearly the same for fine discretization.

However, if we consider all the components of the added mass tensor, which calculation requires vertical and rotational airfoil motion simulation, where solution is unbounded near the sharp edge (Fig. 4(b)), we obtain much coarser result (Table 3).

The scheme $\mathcal{T}^1$ is now approximately 10 time more accurate than $\mathcal{T}^0$, but both schemes provide now not higher than the first order of accuracy due to not enough accuracy of solution reconstruction on the panels that are adjacent to the sharp edge (Fig. 5).

Table 3: Maximal relative errors of the all the added masses estimation for Joukowsky wing airfoil for different number of panels.

N	100	200	400	800	1600	3200
$\delta(\mathcal{T}^0)$	$2.51\cdot10^{-2}$	$1.29\cdot10^{-2}$	$6.88\cdot10^{-3}$	$3.73\cdot10^{-3}$	$2.03\cdot10^{-3}$	$1.11\cdot10^{-3}$
Order	—	(0.96)	(0.91)	(0.88)	(0.87)	(0.87)
$\delta(\mathcal{T}^1)$	$4.55\cdot10^{-3}$	$1.65\cdot10^{-3}$	$7.40\cdot10^{-4}$	$3.51\cdot10^{-4}$	$1.71\cdot10^{-4}$	$8.49\cdot10^{-5}$
Order	—	(1.46)	(1.16)	(1.08)	(1.03)	(1.01)

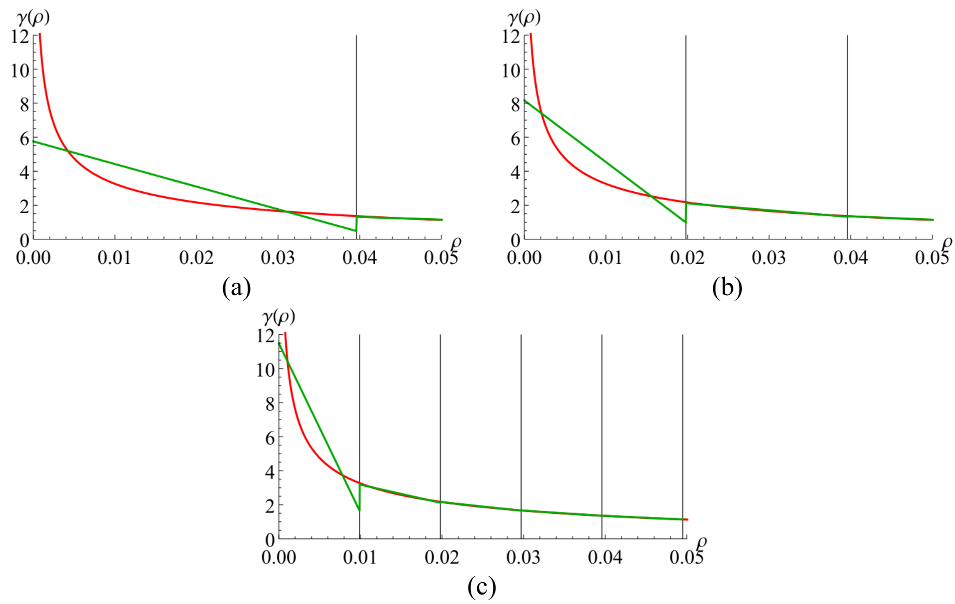

Figure 5: Vortex sheet intensity against the distance to the sharp edge obtained by using the $\mathcal{T}^1$ scheme with piecewise-constant solution representation (green line) and the exact solution (red curve); number of panels $N = 100$ (a); $N = 200$ (b); and $N = 400$ (c); vertical lines correspond to panel endings.

Such an issue cannot be overcome in the framework of the schemes $\mathcal{T}^0$ and $\mathcal{T}^1$ since the solution now belongs to L_1 functional space instead of space containing bounded smooth functions, or piecewise-smooth bounded functions with fixed point of jump discontinuity.

5 NUMERICAL SCHEME WITH SINGULAR BASIS FUNCTIONS

It is seen from Fig. 5 that the scheme $\mathcal{T}^1$ is quite suitable over all the panels except those, which are adjacent to the sharp edge. This put us onto an idea of the modification of this scheme that allows for taking into account singularity of the solution. Let us suggest the following representation for the solution:

$$\gamma(\mathbf{r}) = \left(\gamma_1^0\phi_1^0(\mathbf{r}) + \gamma_1^a\phi_1^a(\mathbf{r})\right) + \sum_{i=2}^{N-1}\left(\gamma_i^0\phi_i^0(\mathbf{r}) + \gamma_i^1\phi_i^1(\mathbf{r})\right) + \left(\gamma_N^0\phi_N^0(\mathbf{r}) + \gamma_N^a\phi_N^a(\mathbf{r})\right), \quad \mathbf{r} \in K, \quad (8)$$

where on the first and N th panels the solution basis functions

$$\phi_1^a(\mathbf{r}) = \frac{L_1^\mu}{s_1(\mathbf{r})^\mu} - \frac{1}{1-\mu}, \qquad \overline{\phi}_N^a(\mathbf{r}) = \frac{L_N^\mu}{\left(L_N - s_N(\mathbf{r})\right)^\mu} - \frac{1}{1-\mu}$$

are introduced instead of linear ones; $s_i(\mathbf{r})$ means the distance from the beginning of the i th panel to the point $\mathbf{r}$. Such choice of basis functions is consistent with the asymptotic behavior of the exact solution (5); the constant $(1-\mu)^{-1}$ is added in order to provide their average value equal to zero.

However, the traditional Galerkin approach, according to which projection functions are equal to basis ones, now does not seem to be suitable. First of all, we note that it is applicable in principle only for $\mu < 1/2$; it means that we can consider only airfoils with corner points, but not with sharp edges, since in the last case the integrals over the first and the N th panels

$$\int_{K_1} \left(\phi_1^a(\mathbf{r})\right)^2 dl_r = \infty, \qquad \int_{K_N} \left(\overline{\phi}_N^a(\mathbf{r})\right)^2 dl_r = \infty,$$

i.e., they do not converge. This follows from the fact that the exact solution for the airfoil with sharp edge $(\mu = 1/2)$ does not belong to L_2 functional space, but belongs to L_1 space.

In order to develop universal algorithm, we use Petrov–Galerkin approach, according to which the set of projection functions differs from set of basis ones. Namely, we use now the same projection functions as in original $\mathcal{T}^1$ scheme: $\left\{\phi_i^0\right\}_{i=1}^N$ and $\left\{\phi_i^1\right\}_{i=1}^N$, i.e., piecewise-constant and piecewise-linear ones. Another advantage of such approach is connected to the computation of the coefficients of the resulting matrix: only $4N$ coefficients should be replaced by new values, while $4N(N-1)$ remain the same as in the matrix arising in the $\mathcal{T}^1$ scheme (note, that the right-hand side remains exactly the same).

The results of the BIE solution obtained by using the suggested scheme (let us denote it $\mathcal{T}_a^1$) for the above considered wing airfoil with corner point are shown in Fig. 6.

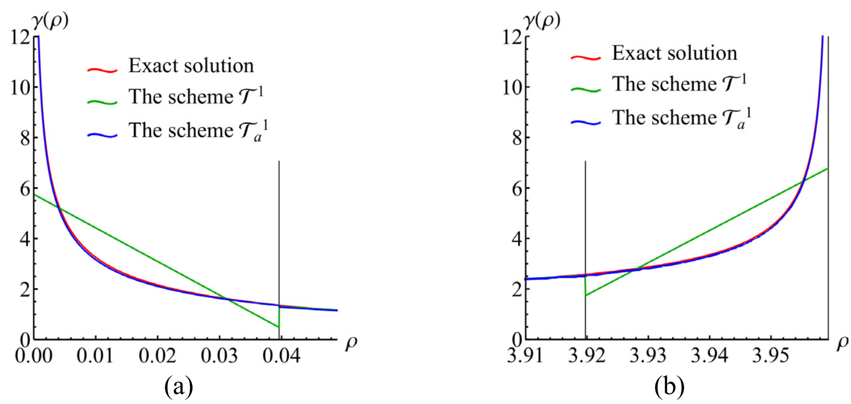

Figure 6: Vortex sheet intensity over the first (a) and the N th (b) panels of the wing airfoil for the surface line discretization into $N = 100$ panels; vertical lines = panel endings.

It is clearly seen that the quality and accuracy of solution reconstruction on the first panel is now much higher than for original $\mathcal{T}^1$ scheme. Over the Nth panel the exact and numerical solutions behavior is quite similar.

Let us now estimate the quality of the developed scheme $\mathcal{T}_a^1$ by estimating the added mass components tensor for the Joukowsky airfoil with sharp edge that was considered above (Fig. 3). The maximal relative error for all the added masses are shown in Table 4.

It is seen that the second order of accuracy is provided due to solution singularity accounting.

Table 4: Maximal relative errors of the all the added masses estimation for Joukowsky wing airfoil for different number of panels.

N	100	200	400	800	1600	3200
$\delta(\mathcal{T}_a^1)$	$4.59\cdot10^{-3}$	$1.19\cdot10^{-2}$	$3.01\cdot10^{-4}$	$7.56\cdot10^{-5}$	$1.89\cdot10^{-5}$	$4.74\cdot10^{-6}$
Order	—	(1.95)	(1.98)	(1.99)	(2.00)	(2.00)

6 CONCLUSION

The problem of the numerical solution of a boundary integral equation of the second kind arising in 2D vortex methods with respect to the intensity of the vortex sheet at the airfoil surface line is considered. In case of the airfoil with a corner point or a sharp edge, the exact solution of the integral equation becomes unbounded, which does not allow the boundary integral equation to be numerically solved with high accuracy using the Galerkin approach with bounded basis functions. A scheme based on the Petrov–Galerkin method is proposed as an original numerical scheme that allows one to reconstruct unbounded solutions. In this scheme, constant basis functions and unbounded basis functions with a known asymptotic behavior are introduced on the panels where the solution is unbounded, on the other panels constant and linear basis functions are used; on all panels, constant and linear functions are chosen as projection functions. The developed scheme allows one to improve the accuracy significantly.

REFERENCES

[1] Cottet, G.-H. & Koumoutsakos, P.D., *Vortex Methods: Theory and Practice*, CUP, 2000.

[2] Lewis, R.I., *Vortex Element Methods for Fluid Dynamic Analysis of Engineering Systems*, Cambridge, 1991.

[3] Branlard, E., *Wind Turbine Aerodynamics and Vorticity-Based Methods: Fundamentals and Recent Applications*, Springer, 2017.

[4] Lifanov, I.K., *Singular Integral Equations and Discrete Vortices*, Utrecht, 1996.

[5] Lifanov, I.K., Poltavsky, L.N. & Vainikko, G., *Hypersingular Equations and their Applications*, CRC Press, 2004.

[6] Kempka, S.N., Glass, M.W., Peery, J.S., Strickland, J.H. & Ingber, M.S., Accuracy considerations for implementing velocity boundary conditions in vorticity formulations. SANDIA report SAND96-0583, 1996.

[7] Kuzmina, K.S. & Marchevskii, I.K., On the calculation of the vortex sheet and point vortices effects at approximate solution of the boundary integral equation in 2D vortex methods of computational hydrodynamics. *Fluid Dyn.*, **54**, pp. 991–1001, 2019.

[8] Kuzmina, K.S., Marchevskii, I.K., Moreva, V.S. & Ryatina E.P., Numerical scheme of the second order of accuracy for vortex methods for incompressible flow simulation around airfoils. *Russ. Aeronaut*., **60**, pp. 398–405, 2017.

[9] Marchevsky, I.K., Kuzmina, K.S. & Soldatova, I.A., Improved algorithm of boundary integral equation approximation in 2D vortex method for flow simulation around curvilinear airfoil. *Mathematics and Mathematical Modeling*, **6**, pp. 22–51, 2018.

[10] Tokaty, G.A., *A History and Philosophy of Fluid Mechanics*, New York, 1994.

[11] Glauert, H., A generalised type of Joukowski aerofoil. *NACA Reports and Memoranda*, **911**, 1924.

[12] Dynnikova, G.Y., Added mass in a model of a viscous incompressible fluid. *Dokl. Phys*., **64**, pp. 397–400, 2019.

[13] Sedov, L.I., *Two-Dimensional Problems in Hydrodynamics and Aerodynamics*, Geneva, 1965.